

$U(1)_A$ symmetry restoration at finite temperature with mesonic correlators

Ryan Bignell,^{a,*} Gert Aarts,^b Chris Allton,^b Benjamin Jäger,^c Seyong Kim,^d
Jon-Ivar Skullerud^{e,a} and Antonio Smecca^{b,f}

^a*School of Mathematics & Hamilton Mathematics Institute, Trinity College, Dublin, Ireland*

^b*Centre for Quantum Fields and Gravity, Department of Physics, Swansea University, Swansea, SA2 8PP, United Kingdom*

^c*Quantum Theory Center (\hbar QTC) & Danish IAS, Department of Mathematics and Computer Science, University of Southern Denmark, 5230, Odense M, Denmark*

^d*Department of Physics, Sejong University, Seoul 143-747, Korea*

^e*Department of Physics, Maynooth University–National University of Ireland Maynooth, County Kildare, Ireland*

^f*INFN, Sezione di Roma Tre, Via della Vasca Navale 84, I-00146 Rome, Italy*

*E-mail: bignellr@tcd.ie, {g.aarts,c.allton}@swansea.ac.uk,
jaeger@imada.sdu.dk, skim@sejong.ac.kr, jonivar.skullerud@mu.ie,
antonio.smecca@roma3.infn.it*

The $U(1)_A$ symmetry of the massless QCD Lagrangian is explicitly broken in the quantised theory by the anomaly. It may be effectively restored at some finite temperature, which would have important consequences for the order of the chiral transition and the QCD phase diagram. It has been argued in the literature that one way to probe the effective restoration of $U(1)_A$ is to check for the degeneracy of pseudoscalar and flavour non-singlet scalar correlators. In this work, we consider a new method of examining this degeneracy based upon hadron correlation functions on the anisotropic FASTSUM ensembles. The anisotropic nature and our newest Generation 3 ensembles aid in a determination of the effective restoration of the $U(1)_A$ symmetry which we find to be $T_{U(1)_A} \sim 320$ MeV, well above the chiral transition temperature, which is $T_{pc} \sim 180$ MeV for our choice of Wilson-Clover fermions.

*The 42nd International Symposium on Lattice Field Theory (LATTICE2025)
2-8 November 2025
Tata Institute of Fundamental Research, Mumbai, India*

*Speaker

1. Introduction

While the massless QCD Lagrangian is invariant under the symmetry $SU(n_f)_L \times SU(n_f)_R \times U(1)_V \times U(1)_A$ (for n_f flavours), the $SU(n_f)_L \times SU(n_f)_R$ chiral symmetry is spontaneously broken at zero temperature and the $U(1)_A$ symmetry is explicitly broken by quantisation [1, 2]. The chiral symmetry is restored at some finite temperature, while the $U(1)_A$ symmetry is thought to be effectively restored — it remains explicitly broken but the breaking effects are suppressed [3]. The pseudo-critical temperature for chiral symmetry restoration is well known to be about $T_{pc} \simeq 154$ MeV [4–6] for physical quark masses. In contrast, the effective restoration of the $U(1)_A$ symmetry is still not settled [7, 8]. It is becoming evident that $U(1)_A$ symmetry is likely not (effectively) restored at the chiral transition temperature, but where and if the restoration occurs is yet unclear [9–12].

The restoration of $U(1)_A$ symmetry should be manifest [13–15] at the level of mesonic correlation functions, specifically through the degeneracy of the pseudoscalar (π) and the flavour non-singlet scalar meson (δ) channels. This can be examined through the spectral density of the Dirac operator [16, 17]. Due to our choice of Wilson-Clover [18] fermions, which makes direct spectral density studies difficult, we instead consider the correlation functions themselves.

The most common approach using mesonic correlators is to consider the susceptibilities

$$\chi_\pi = \sum_{\vec{x}, \tau} G_\pi(\vec{x}, \tau) \quad \text{and} \quad \chi_\delta = \sum_{\vec{x}, \tau} G_\delta(\vec{x}, \tau), \quad (1)$$

where $G_{[\pi, \delta]}(x)$ are the pseudoscalar and flavour non-singlet scalar two-point correlation function respectively. The difference in susceptibilities $\chi_\pi - \chi_\delta$ is used to study the restoration. These susceptibilities are used in an attempt to remove ultraviolet divergences [19, 20], which even good chiral actions such as Domain Wall Fermions suffer from [21]. In order to further reduce the effect of these ultraviolet – or short distance – artefacts we introduce two additional methods. In combination with the high-temperature anisotropic FASTSUM ensembles, these enable an examination of where $U(1)_A$ symmetry is effectively restored at high temperature.

2. Ensembles

In this work we use the latest FASTSUM “Generation 3” ensembles [22, 23]. These are anisotropic ensembles with the temporal lattice spacing a_τ a factor of $\xi = a_s/a_\tau \sim 7$ times smaller than the spatial lattice spacing. This allows a fine spread of temperatures using the fixed-scale approach, wherein the temperature is changed by changing the temporal extent of the lattice, $T = 1/(a_\tau N_\tau)$. Following the HadSpec Collaboration [24, 25] we use an $\mathcal{O}(a^2)$ improved gauge action and an $\mathcal{O}(a)$ improved Wilson-Clover fermion action.

The light quark mass is tuned to closely reproduce the pion mass of our previous “Generation 2” ensembles [26–28] giving $m_\pi = 378(1)$ MeV with a near physical strange quark mass. The spatial lattice spacing is $a_s = 0.10796(57)$ fm with anisotropy $\xi = a_s/a_\tau = 7.0161(94)$. The

N_τ	256	128	112	96	80	76	72	68	64	56	48	40	36	32	24
$T(\text{MeV})$	50	100	114	133	160	169	178	188	200	229	267	320	356	400	534

Table 1: Generation 3 ensembles showing the temporal extent N_τ and the corresponding temperature.

pseudocritical temperature, measured via the chiral condensate, is $T_{pc} \sim 180$ MeV. The Generation 3 ensembles span a broad range of temperatures with $T \in [50, 534]$ MeV as shown in Table 1. The zero-temperature ensemble, $N_\tau = 256$, has spatial extent $N_s = 24$, while for the others it is $N_s = 32$.

3. Results using local correlation functions

Here we discuss the three methods used to examine the degeneracy of the pseudoscalar and flavour non-singlet scalar mesons using “local-local” (point source and sink) correlators.

3.1 Standard Definition

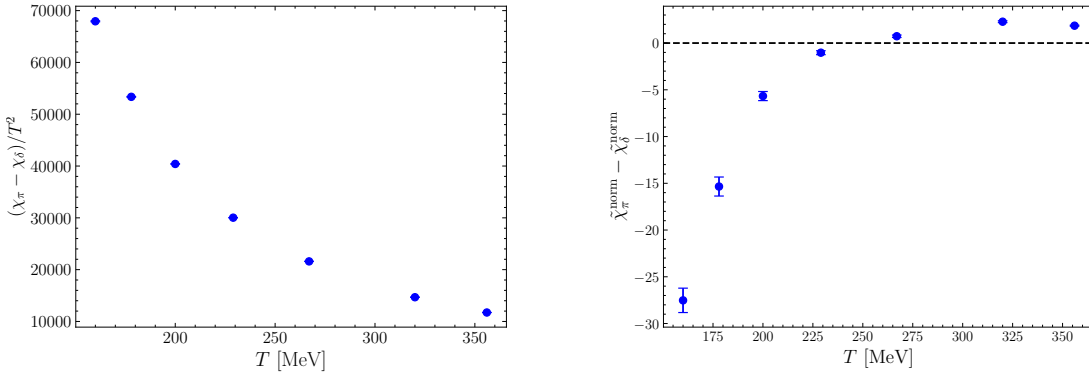


Figure 1: **Left:** Subtracted susceptibilities $\chi_\pi - \chi_\delta$, see Eq. (1). **Right:** Subtracted normalised susceptibilities $\tilde{\chi}_\pi^{\text{norm}} - \tilde{\chi}_\delta^{\text{norm}}$, see Eq. (2). The correlator has been normalised at the mid-point first and summed starting at $\tau_{\min} T = 0.2$.

The results using the standard definition (1) are shown in Fig. 1 (left). Although there is a clear decrease in the difference of susceptibilities as the temperature increases, the difference remains far from zero, suggesting that there is no degeneracy. The susceptibilities here are unrenormalised. This is because the operators used do not (necessarily) have the same overlap with the pseudoscalar/scalar states and hence subtraction will not show degeneracy. Furthermore, any short-distance effects due to excited states and the Wilson term are unmitigated here.

3.2 Normalise and cutoff

The second definition introduces a short-distance cutoff: each (temporal) correlator is normalised at its mid-point and only summed after a few time steps to reduce short-distance artefacts. We first define, for the remainder of this manuscript, $G_{[\pi,\delta]}(\tau) = \sum_{\vec{x}} G_{[\pi,\delta]}(\vec{x}, \tau)$ and then construct the susceptibility

$$\tilde{\chi}_{[\pi,\delta]}^{\text{norm}} = \sum_{\tau=\tau_{\min}}^{N_\tau/2} \frac{G_{[\pi,\delta]}(\tau)}{G_{[\pi,\delta]}(N_\tau/2)}. \quad (2)$$

We then take the difference $\tilde{\chi}_\pi^{\text{norm}} - \tilde{\chi}_\delta^{\text{norm}}$ as before. The improvement here is twofold – first the dependence on the overlap of the energy states in the operators is removed by normalising

with respect to the mid-point of the correlator, where the ground state dominates, and second, short-distance effects are removed by introducing a short-distance temporal cut-off τ_{\min} . Hence we have enhanced the sensitivity of $\tilde{\chi}^{\text{norm}}$ to infrared effects relevant to the (effective) restoration of $U(1)_A$ symmetry. The difference in the resulting susceptibilities is shown in Fig. 1 (right). Here the sum starts from $\tau_{\min} T = 0.2$. This difference now approaches (and crosses) zero showing (effective) $U(1)_A$ symmetry restoration. Remnant artefacts due to the Wilson term may still be present on ensembles with short temporal extent. This contributes to the rise of the susceptibility difference above zero. While care must be taken when choosing τ_{\min} , we find that in this setup $U(1)_A$ symmetry is effectively restored at $T \gtrsim 225$ MeV.

3.3 Normalised Ratio

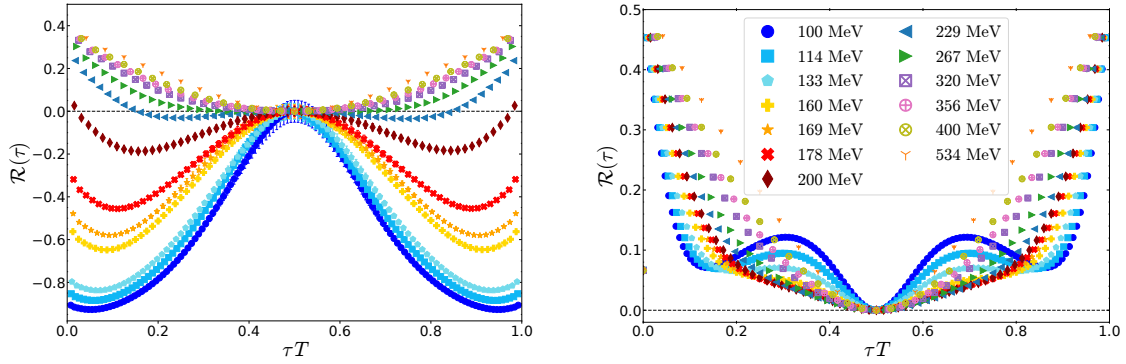


Figure 2: **Left:** Ratio of normalised correlators $\mathcal{R}(\tau)$, see Eq. (3). Note that the data corresponds to the legend in the figure on the right, with the temperature increasing vertically along the left-hand side of the plot. **Right:** Ratio $\mathcal{R}(\tau)$ for free Wilson correlators on lattices of the same dimensions as Generation 3.

The final method we consider is to construct a ratio of the difference of normalised correlators [27, 29, 30]

$$\mathcal{R}(\tau) = \frac{\tilde{G}_\pi(\tau) - \tilde{G}_\delta(\tau)}{\tilde{G}_\pi(\tau) + \tilde{G}_\delta(\tau)}, \quad (3)$$

where $\tilde{G}(\tau)$ is the mid-point normalised correlator $\tilde{G}(\tau) = G(\tau) / G(N_\tau/2)$. This ratio is constructed such that it is close to ± 1 when the correlators are non-degenerate and the ground state masses differ substantially, and zero when they are exactly degenerate. The ratio vanishes at $\tau = N_\tau/2$ by construction. Since $m_\pi \ll m_\delta$, non-degeneracy is indicated by values close to -1 . The mid-point normalisation handles any relative difference in the operator overlap. With different mesonic channels, this ratio has previously been used to examine the chiral transition temperature [27, 30]

This ratio is presented in Fig. 2 (left). The ratio is, of course, symmetric for mesonic correlators. It is clear that as the temperature increases, in the intermediate region of $\tau T \sim [0.2, 0.4]$ it gets closer to zero. At the edge of the lattice there is an upwards curvature. This behaviour can be understood through consideration of free Wilson correlators (for details, see Ref. [30]) as in Fig. 2 (right). Here the influence of artefacts due to the Wilson term is manifest at the edges of the lattice.

4. Smear Ratio

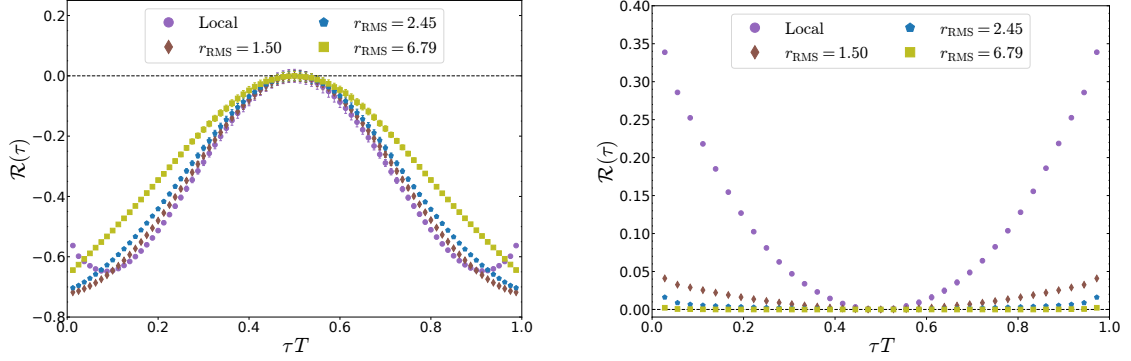


Figure 3: Ratio $\mathcal{R}(\tau)$, see Eq. (3), for four different smearing radii (including none) at $T \sim 160$ MeV (left) and $T \sim 356$ MeV (right). Note that the vertical scales are different.

Up to now, we considered local-local correlators only. To reduce the impact of the artefacts due to the Wilson term, we consider now standard Gaussian smeared correlators [31, 32]. Source and sink smearing is a common technique used to reduce overlap with heavy excited states, some of which are due to the nature of the Wilson-Clover action.

To tune the amount of smearing used we compare the resulting ratio (3) for four different levels of smearing (including none) in Fig. 3 at two different temperatures. The amount of smearing is described by the root-mean-square radius of the Gaussian profile on a free point source. The $r_{\text{RMS}} = 6.79$ profile was chosen to match the one previously optimised for nucleon and charm baryon spectroscopy in Refs. [27, 32]; the other values were chosen to be smaller in radii.

From Fig. 3 it is evident that at very high temperatures ($T \sim 356$ MeV) that there is little difference between the smeared correlators, but that at lower temperatures ($T \sim 160$ MeV) larger differences remain (note the vertical scale in the left and right plots is different). Close to the mid-point of the correlator, the ground state should be dominant and the smeared correlators should resemble the “local” or unsmeared correlator and this is observed for all but the $r_{\text{RMS}} = 6.79$ correlators. Hence we discard these. Of the remaining correlators, we select the $r_{\text{RMS}} = 2.45$ correlator corresponding to $\kappa = 1.96$, $n = 6$ in our smearing algorithm [31, 32], as it most effectively eliminates the upwards curve at short temporal separation.

4.1 Integrated Ratio

The ratio constructed in Eq. (3) is useful as it allows an examination of the influence of Wilson artefacts and the desired degeneracy (or lack thereof), but it is difficult to use it to determine at what temperature degeneracy occurs. Hence in the spirit of the original definition (1) of the susceptibilities, we construct the integrated (summed) ratio

$$R(\tau_{\min}, N_{\tau}/2; T) = \frac{\sum_{\tau_{\min}}^{N_{\tau}/2} \mathcal{R}(\tau, T) / \sigma_{\mathcal{R}}^2(\tau, T)}{\sum_{\tau_{\min}}^{N_{\tau}/2} 1 / \sigma_{\mathcal{R}}^2(\tau, T)}, \quad (4)$$

where $\mathcal{R}(\tau, T)$ is the ratio of Eq. (3) and $\sigma_{\mathcal{R}}(\tau, T)$ the corresponding uncertainty. As in the definition of Eq. (2), there is some freedom in the choice of τ_{\min} but we find that the use of smeared

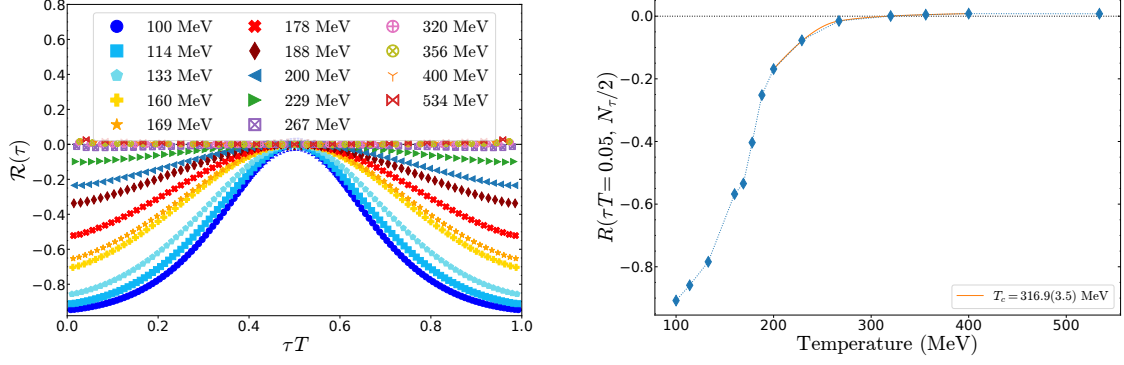


Figure 4: Left: Ratio $\mathcal{R}(\tau)$, see Eq. (3), using smeared correlators. Right: Corresponding integrated ratio R , see Eq. (4). The orange curve is a spline interpolation used to find the intercept of the curve with zero.

correlators greatly reduces this effect. This integrated ratio inherits the properties of the underlying ratio, namely that degeneracy is evident by a zero value and non-degeneracy by a value close to -1 .

In Fig. 4 (left) we show the ratio of Eq. (3) using smeared correlators. Note how the introduction of smearing has greatly reduced the upwards inflection at the edges of the lattice in comparison to the unsmearing correlators and that the ratio now remains close to zero once degeneracy has been reached. It is important to note that all the ratio plots are plotted as a function of τT and hence an ensemble at a higher temperature has fewer points.

The integrated ratio of Eq. (4), using the smeared correlator data, is shown in Fig. 4 (right). Here the sum is taken from $\tau_{\min} T = 0.05$; hence τ_{\min} is different for each temperature. The correlators are clearly not degenerate at the chiral transition temperature $T_{pc} \sim 180$ MeV, but instead become degenerate at a much higher temperature. To determine the temperature at which this occurs, a cubic spline interpolation is performed and the intersection with 0 is found. For this data, this temperature is $T_{U(1)_A} = 317(4)$ MeV, significantly above T_{pc} . The uncertainty of 4 MeV is purely statistical; a fuller determination of systematic uncertainties is planned.

Although the integrated ratio becomes slightly non-zero and crosses zero after $T_{U(1)_A}$, this is not too concerning. Even though the smearing has mitigated artefacts due to the Wilson term, the fermion action still explicitly breaks chiral symmetry – the impact of this seems slight in the vector/axial-vector integrated ratio as we recently examined [30]. Our set-up is at a moderate quark mass ($m_\pi \sim 380$ MeV) and here we clearly see the effective restoration of $U(1)_A$ symmetry.

5. Conclusions and Future Work

We studied the effective restoration of $U(1)_A$ symmetry on Generation 3 FASTSUM ensembles with Wilson-Clover fermions, with a pion mass of $m_\pi \sim 380$ MeV and an anisotropy of $\xi \sim 7$, by analysing an integrated ratio of smeared π and δ correlators. We found that this symmetry is effectively restored at $T = 317(4)$ MeV, well above the chiral transition temperature $T_{pc} \sim 180$ MeV.

An advantage of the anisotropic FASTSUM ensembles is that they span a broad range of temperatures, both below and above T_{pc} . This, combined with the anisotropic nature which enables temporal correlation functions with many points, allows a novel investigation of the susceptibilities

before they are summed. In particular, the use of the (integrated) ratio has allowed for a detailed understanding of systematic effects associated with the Wilson term and the choice of τ_{\min} . This work confirms the lack of $U(1)_A$ restoration at T_{pc} and provides a new way to determine the transition temperature.

In the future we will include the other FASTSUM ensembles, Generation 2 [26–28] and 2L [27, 33, 34], to give an estimate of systematic effects associated with the pion mass and the anisotropy. It is interesting that for our ensembles the effective restoration temperature for $U(1)_A$ is close to the transition temperature found in Ref. [35] via centre vortices, indicating the possible existence of a third high-temperature phase of QCD matter [35–37]. We also look forward to applying these methods to the puzzle of chiral spin symmetry [38–41].

Software and Data

The Generation 3 ensembles were generated using OPENQCD-FASTSUM [42]. They will be made available at some point in the future in accordance with FASTSUM’s sharing policy. The correlators and analysis workflow will be made available along with a future publication. This analysis makes extensive use of the PYTHON packages GVAR [43], MATPLOTLIB and NUMPY as well as a jackknife analysis implemented in FORTRAN using the FORTRAN-PACKAGE-MANAGER [44, 45].

Acknowledgements

This work is supported by STFC grant ST/X000648/1. GA is supported by a Royal Society Leverhulme Trust Senior Research Fellowship. RB acknowledges support from a Science Foundation Ireland Frontiers for the Future Project award with grant number SFI-21/FFP-P/10186. SK is supported by the National Research Foundation of Korea through the grant, NRF-2008-000458. We acknowledge the EuroHPC Joint Undertaking for awarding the projects EHPC-EXT-2023E01-010 and EXT-2025E01-079 access to LUMI-C and LUMI-G, Finland. This work used the DiRAC Data Intensive service (DIaL2 & DIaL) at the University of Leicester, managed by the University of Leicester Research Computing Service on behalf of the STFC DiRAC HPC Facility (www.dirac.ac.uk). The DiRAC service at Leicester was funded by BEIS, UKRI and STFC capital funding and STFC operations grants. This work used the DiRAC Extreme Scaling service (Tesseract) at the University of Edinburgh, managed by the Edinburgh Parallel Computing Centre on behalf of the STFC DiRAC HPC Facility (www.dirac.ac.uk). The DiRAC service at Edinburgh was funded by BEIS, UKRI and STFC capital funding and STFC operations grants. This work was performed using PRACE resources at Joliot-Curie (Irene) hosted in Rome and Hawk hosted by HLRS Stuttgart. We acknowledge the support of the Supercomputing Wales project, which is part-funded by the European Regional Development Fund (ERDF) via Welsh Government.

References

- [1] J.S. Bell and R. Jackiw, *A pcac puzzle: $\pi^0 \rightarrow \gamma\gamma$ in the σ -model*, *Il Nuovo Cimento A (1965-1970)* **60** (1969) 47.
- [2] S.L. Adler, *Axial-vector vertex in spinor electrodynamics*, *Phys. Rev.* **177** (1969) 2426.

- [3] A.G. Nicola, *Light quarks at finite temperature: chiral restoration and the fate of the $U(1)_A$ symmetry*, *Eur. Phys. J. ST* **230** (2021) 1645 [2012.13809].
- [4] HotQCD collaboration, *Chiral crossover in QCD at zero and non-zero chemical potentials*, *Phys. Lett. B* **795** (2019) 15 [1812.08235].
- [5] S. Borsanyi, Z. Fodor, J.N. Guenther, R. Kara, S.D. Katz, P. Parotto et al., *QCD Crossover at Finite Chemical Potential from Lattice Simulations*, *Phys. Rev. Lett.* **125** (2020) 052001 [2002.02821].
- [6] R.V. Gavai, M.E. Jaensch, O. Kaczmarek, F. Karsch, M. Sarkar, R. Shanker et al., *Aspects of the chiral crossover transition in (2+1)-flavor QCD with Möbius domain-wall fermions*, *Phys. Rev. D* **111** (2025) 034507 [2411.10217].
- [7] A. Lahiri, *Aspects of finite temperature QCD towards the chiral limit*, *PoS LATTICE2021* (2022) 003 [2112.08164].
- [8] S. Borsanyi and P. Parotto, *The QCD phase diagram*, 2512.08843.
- [9] B.B. Brandt, A. Francis, H.B. Meyer, O. Philipsen, D. Robaina and H. Wittig, *On the strength of the $U_A(1)$ anomaly at the chiral phase transition in $N_f = 2$ QCD*, *JHEP* **12** (2016) 158 [1608.06882].
- [10] JLQCD collaboration, *Study of the axial $U(1)$ anomaly at high temperature with lattice chiral fermions*, *Phys. Rev. D* **103** (2021) 074506 [2011.01499].
- [11] O. Kaczmarek, L. Mazur and S. Sharma, *Eigenvalue spectra of QCD and the fate of $U_A(1)$ breaking towards the chiral limit*, *Phys. Rev. D* **104** (2021) 094518 [2102.06136].
- [12] S. Dentinger, O. Kaczmarek and A. Lahiri, *Screening masses towards chiral limit*, *Acta Phys. Polon. Supp.* **14** (2021) 321 [2102.09916].
- [13] E.V. Shuryak, *Which chiral symmetry is restored in hot QCD?*, *Comments Nucl. Part. Phys.* **21** (1994) 235 [hep-ph/9310253].
- [14] T.D. Cohen, *The High temperature phase of QCD and $U(1)_A$ symmetry*, *Phys. Rev. D* **54** (1996) R1867 [hep-ph/9601216].
- [15] T.D. Cohen, *The Spectral density of the Dirac operator above T_c* , in *APCTP Workshop on Astro-Hadron Physics: Properties of Hadrons in Matter*, pp. 100–114, 10, 1997 [nucl-th/9801061].
- [16] V. Dick, F. Karsch, E. Laermann, S. Mukherjee and S. Sharma, *Microscopic origin of $U_A(1)$ symmetry violation in the high temperature phase of QCD*, *Phys. Rev. D* **91** (2015) 094504 [1502.06190].
- [17] S. Aoki, H. Fukaya and Y. Taniguchi, *Chiral symmetry restoration, eigenvalue density of Dirac operator and axial $U(1)$ anomaly at finite temperature*, *Phys. Rev. D* **86** (2012) 114512 [1209.2061].

- [18] B. Sheikholeslami and R. Wohlert, *Improved Continuum Limit Lattice Action for QCD with Wilson Fermions*, *Nucl. Phys. B* **259** (1985) 572.
- [19] HOTQCD collaboration, *The chiral transition and $U(1)_A$ symmetry restoration from lattice QCD using Domain Wall Fermions*, *Phys. Rev. D* **86** (2012) 094503 [1205.3535].
- [20] JLQCD collaboration, *Axial $U(1)$ symmetry, topology, and Dirac spectra at high temperature in $N_f = 2$ lattice QCD*, *PoS CD2018* (2019) 085 [1908.11684].
- [21] G. Cossu, S. Aoki, H. Fukaya, S. Hashimoto, T. Kaneko, H. Matsufuru et al., *Finite temperature study of the axial $U(1)$ symmetry on the lattice with overlap fermion formulation*, *Phys. Rev. D* **87** (2013) 114514 [1304.6145].
- [22] J.-I. Skullerud, G. Aarts, C. Allton, M.N. Anwar, R. Bignell, T. Burns et al., *Approaching the continuum with anisotropic lattice thermodynamics*, *J. Subatomic Part. Cosmol.* **4** (2025) 100258 [2510.02954].
- [23] G. Aarts, C. Allton, M.N. Anwar, R. Bignell, T. Burns, S. Hands et al., “FASTSUM generation 3 anisotropic Wilson-Clover ensembles.” In preparation.
- [24] HADRON SPECTRUM collaboration, *First results from 2+1 dynamical quark flavors on an anisotropic lattice: Light-hadron spectroscopy and setting the strange-quark mass*, *Phys. Rev. D* **79** (2009) 034502 [0810.3588].
- [25] R.G. Edwards, B. Joó and H.-W. Lin, *Tuning for Three-flavors of Anisotropic Clover Fermions with Stout-link Smearing*, *Phys. Rev. D* **78** (2008) 054501 [0803.3960].
- [26] G. Aarts, C. Allton, A. Amato, P. Giudice, S. Hands and J.-I. Skullerud, *Electrical conductivity and charge diffusion in thermal QCD from the lattice*, *JHEP* **02** (2015) 186 [1412.6411].
- [27] G. Aarts, C. Allton, J. Glesaaen, S. Hands, B. Jäger, S. Kim et al., *Properties of the QCD thermal transition with $N_f=2+1$ flavors of Wilson quark*, *Phys. Rev. D* **105** (2022) 034504 [2007.04188].
- [28] G. Aarts, C. Allton, A. Amato, R. Bignell, T.J. Burns, D. De Boni et al., *FASTSUM Generation 2 Anisotropic Thermal Lattice QCD Gauge Ensembles*, Zenodo (Oct., 2023), 10.5281/zenodo.8403827.
- [29] S. Datta, S. Gupta, M. Padmanath, J. Maiti and N. Mathur, *Nucleons near the QCD deconfinement transition*, *JHEP* **02** (2013) 145 [1212.2927].
- [30] A. Smecca, G. Aarts, C. Allton, R. Bignell, B. Jäger, S.-i. Nam et al., *Curvature of the pseudocritical line in the QCD phase diagram from mesonic lattice correlation functions*, *Phys. Rev. D* **112** (2025) 114509 [2412.20922].
- [31] S. Güsken, *A Study of smearing techniques for hadron correlation functions*, *Nucl. Phys. B Proc. Suppl.* **17** (1990) 361.

- [32] G. Aarts, C. Allton, M.N. Anwar, R. Bignell, T.J. Burns, B. Jäger et al., *Non-zero temperature study of spin 1/2 charmed baryons using lattice gauge theory*, *Eur. Phys. J. A* **60** (2024) 59 [2308.12207].
- [33] G. Aarts, C. Allton, R. Bignell, T.J. Burns, S.C. García-Masaraque, S. Hands et al., *Open charm mesons at nonzero temperature: results in the hadronic phase from lattice QCD*, 2209.14681.
- [34] G. Aarts, C. Allton, M.N. Anwar, R. Bignell, T.J. Burns, S. Chaves Garcia-Masaraque et al., *FASTSUM Generation 2L Anisotropic Thermal Lattice QCD Gauge Ensembles*, Zenodo (Feb., 2024), 10.5281/zenodo.10636046.
- [35] J.A. Mickley, C. Allton, R. Bignell and D.B. Leinweber, *Center vortex evidence for a second finite-temperature QCD transition*, *Phys. Rev. D* **111** (2025) 034508 [2411.19446].
- [36] A. Alexandru and I. Horváth, *Possible New Phase of Thermal QCD*, *Phys. Rev. D* **100** (2019) 094507 [1906.08047].
- [37] A.Y. Kotov, M.P. Lombardo and A. Trunin, *Topological observables and θ dependence in high temperature QCD from lattice simulations*, *JHEP* **09** (2025) 045 [2502.15407].
- [38] C. Rohrhofer, Y. Aoki, G. Cossu, H. Fukaya, C. Gattringer, L.Y. Glozman et al., *Symmetries of spatial meson correlators in high temperature QCD*, *Phys. Rev. D* **100** (2019) 014502 [1902.03191].
- [39] T.-W. Chiu, *Symmetries in High-Temperature Lattice QCD with (u, d, s, c, b) Optimal Domain-Wall Quarks*, *Symmetry* **17** (2025) 700 [2411.16705].
- [40] L.Y. Glozman, *Chiral spin symmetry*, 2510.14084.
- [41] O. Philipsen, *Emergent chiral spin symmetry, non-perturbative dynamics and thermoparticles in hot QCD*, 2512.18830.
- [42] J.R. Glesaaen and B. Jäger, *openqcd-fastsum*, Apr., 2018. 10.5281/zenodo.2216356.
- [43] P. Lepage, C. Gohlke and D. Hackett, *gplepage/gvar: gvar version 13.1.5*, Jan., 2025. 10.5281/zenodo.14783421.
- [44] M. Curcic, O. Certik, B. Richardson, S. Ehlert, L. Kedward, A. Markus et al., *Toward modern fortran tooling and a thriving developer community*, *CoRR* **abs/2109.07382** (2021) [2109.07382].
- [45] L. Kedward, B. Aradi, O. Certik, M. Curcic, S. Ehlert, P. Engel et al., *The state of fortran, Computing in Science and Engineering* **24** (2022) 63 [2203.15110].